International Journal of Mechanical, Industrial and Aerospace Sciences
ISSN: 2517-9950
Vol:5, No:2, 2011

Optimization Approach on Flapping Aerodynamic Characteristics of Corrugated Airfoil

Wei-Hsin Sun, Jr-Ming Miao, Chang-Hsien Tai, and Chien-Chun Hung

***Abstract*—**The development of biomimetic micro-aerial-vehicles (MAVs) with flapping wings is the future trend in military/domestic field. The successful flight of MAVs is strongly related to the understanding of unsteady aerodynamic performance of low Reynolds number airfoils under dynamic flapping motion. This study explored the effects of flapping frequency, stroke amplitude, and the inclined angle of stroke plane on lift force and thrust force of a bio-inspiration corrugated airfoil with 3^3 full factorial design of experiment and ANOVA analysis. Unsteady vorticity flows over a corrugated thin airfoil executing flapping motion are computed with time-dependent two-dimensional laminar incompressible Reynolds-averaged Navier-Stokes equations with the conformal hybrid mesh. The tested freestream Reynolds number based on the chord length of airfoil as characteristic length is fixed of 10^3. The dynamic mesh technique is applied to model the flapping motion of a corrugated airfoil. Instant vorticity contours over a complete flapping cycle clearly reveals the flow mechanisms for lift force generation are dynamic stall, rotational circulation, and wake capture. The thrust force is produced as the leading edge vortex shedding from the trailing edge of airfoil to form a reverse von Karman vortex. Results also indicated that the inclined angle is the most significant factor on both the lift force and thrust force. There are strong interactions between tested factors which mean an optimization study on parameters should be conducted in further runs.

***Keywords*—**biomimetic, MAVs, aerodynamic, ANOVA analysis.

I. Introduction

THIS flapping motion of flexible wings has been considered one of the most graceful and efficient kinds of animal locomotion [1]. The insects and birds use the flapping wings for hovering and forward flight. Since 1992, the Defense Air-Borne Reconnaissance Office (DARO) supports a DARPA initiative project to develop a micro-aerial-vehicle (MAV). The design, analysis, fabrication and test of the performance of MAVs are becoming increasingly import ant due to it can be regarded as small and mobile units operating in severe environments such as urban areas or unconventional operations anywhere. Currently, MAVs are classified as fixed wing, rotating wing or flapping wing MAV. Even the design concepts of flapping MAVs are inspired from observations on the flight behavior of insects and birds. There are great challenges in the development of flapping wing MAV because the unsteady low Reynolds number aerodynamic characteristics of flapping wings are still unclear.

The Knoller-Betz effect seems the first theory to explain the flow mechanism on generation of lift/thrust force due to plunge motion of airfoil with variation of effective attack angle. Water-tunnel flow visualization experiments on flapping symmetric airfoils such as NACA0012 and NACA0014 have been conducted by Triantafyllou et al. [2], Lai and Platzer [3] and Jones et al. [4], which provide information on the formation of thrust-indicative wake with a certain combinations of reduced frequency and heaving stroke. Anderson et al. [5] found that the phase angle between the periodic pitch and plunge motions plays a significant role in producing maximum thrust force.

To understand the flow mechanism on lift force generation, Ellington's group [6] conducted a series of wind-tunnel experiments on flapping wings with flow visualization method and force balance gauges. Their observations indicated that the effects of leading edge vortex and dynamic stall both contributed to the lift force since the attack angle of wing is continuously changed in up-stroke and down-stroke flapping stage. Dickinson classified the flow mechanisms for lift force generation of insects are dynamic stall, rotational circulation and wake capture [7]. Recently, several works had implemented the theory of low Reynolds number unsteady flight aerodynamics into the development of bio-inspired MAV [8]–[10]. On the computational aspect, Navier-Stokes studies have been performed and focused on the aerodynamic characteristic of a single rigid airfoil in freestream with oscillation mode of pure pitch [11] or coupled heave and pitch [12]–[16]. Most researches have used symmetrical NACA4 series airfoils in their works, Wang' group [17], [18] intended to employ the thin elliptic airfoils because they are interested on the dragonfly's wings aerodynamic characteristics. However, an optic microscope picture shows that the cross-section of dragonfly's wing is not similar to elliptic shape but corrugated

Jr-Ming Miao Author is with the Department of Materlals Engineering, National Pingtung University of Science and Technology, Taiwan, R.O.C (corresponding author to provide phone: +886-8-7703202#7566;e-mail: jmmiao@mail.npust.edu.tw).

Wei-Hsin Sun Author is with the School of Defense Science Studies, Chung Cheng Institute of Technology, National Defense University , Taiwan, R.O.C (e-mail: sun1@hotmail.com.tw).

Chang-Hsien Tai Author is with the Department of Vehicle Engineering, National Pingtung University of Science and Technology, Taiwan, R.O.C (e-mail: chtai@mail.npust.edu.tw).

Chien-Chun Hung Author is with the Department of Mechatronic, Energy and Aerospace Engineering Chung Cheng Institute of Technology, National Defense University, Taiwan, R.O.C (e-mail: hung@ndu.edu.tw).

one. Tamai et al. [19]conducted the PIV measurements on velocity distributions with several types of airfoils as GA(W)-1 airfoil, flat plate, and corrugated airfoil by considered the effect of attack angle and Reynolds number. Their results indicated that the corrugated airfoil can suppress the large-scale leading edge vortex formation at large attack angle. Therefore, the aerodynamic performance of corrugated airfoil is superior to the other two types of airfoil at such low Reynolds number.

The published literature contains none of studies about the unsteady aerodynamic behavior of a corrugated airfoil executing flapping motion. Consequently, the objective of present work is to investigate the thrust force and lift force generated by the corrugated airfoil under different flapping parameter configurations of frequency, inclined angle of stroke plane and stroke amplitude. Design of Experiment (DOE) methodology and statistic analysis of variance both are employed to find out the optimum combination of operational parameters on generation of maximum lift force or maximum thrust force. The response surfaces and associated regression model are also constructed to identify the significant factor and interactions between factors. Vorticity contours over a complete cycle of flapping motion are plotted to explain the unsteady flow mechanisms generating the lift force and thrust force. The freestream Reynolds number is fixed of 10^3, which is the typical regime of a flapping MAV.

II. Numerical Methodology

A 3^3 full-factorial design method, at three levels and three factors, has been performed in order to investigate the main and interaction effects of operational parameters on unsteady aerodynamic performance of single flapping corrugated airfoil. The factors considered in this study are the flapping frequency, the inclined angle of stroke plane and the stroke amplitude. The unsteady lift/thrust forces are obtained by solving the unsteady laminar Navier-Stokes equations with the conformal hybrid mesh.

A. Navier-Stokes solver

The working fluid is air and the motion of corrugated airfoil is governed by the two-dimensional time-dependent incompressible Reynolds-averaged Navier-Stoke's equations coupled with the dynamic mesh motions. The time-dependent incompressible Navier-Stokes equations including of continuity equation and momentum equation as:

$$(\nabla \bullet \vec{u}) = 0 \tag{1}$$

$$\frac{\partial \vec{u}}{\partial t} + (\vec{u} \bullet \nabla)\vec{u} = -\frac{\nabla p}{\rho} + \upsilon \nabla^2 \vec{u} \tag{2}$$

where $\vec{u}$ is the velocity vector, p is the pressure, υ is the kinematic viscosity and ρ is the density of air.

The governed equations are solved by the FLUENT@ 12.1.06 software based on the control volume method. The staggered, transient pressure-based solver is employed due to the flow field is varied (especially around the airfoil) during the cyclical plunge and pitch motions of a corrugated airfoil. In governed equations, the convection flux term is discretized with the third-order QUICK scheme, while the diffusion flux term is discretized with the central differencing scheme. As for the coupling of velocity and the pressure in the momentum equations, the SIMPLEC (semi-implicit method for pressure-linked equations consistent) algorithm is used. The AMG (algebraic multi-grid) scheme is also implemented for acceleration of convergence of all scalar variables during each time interval. Due to the constraint of hybrid dynamic mesh system, the implicit method in time accuracy for all runs is only the first-order accuracy. To model the flapping motion of the corrugated airfoil with various operational parameters, present study adopts the dynamic mesh technique instead of the overset grid technique. Besides, the temporal grid deformation is governed by the Geometric Conservation Law (GCL) in each time interval.

B. Computational grids and boundary conditions

Fig. 1(a) is a close-up illustration to present the conformal hybrid mesh system employed for the aerodynamic modeling of inclined flapping motion of corrugated airfoil with prescribed trajectory. Following grid independent and computational domain studies, the final computational domain is composed of 14160 inner quadrilateral cells and 36514 outer triangular cells. The rectangular computation domain is composed with length of $92c_m$ and width of $70c_m$. The center of corrugated airfoil is located $22c_m$ away from the left side of computational domain, shown in Fig. 1(b).

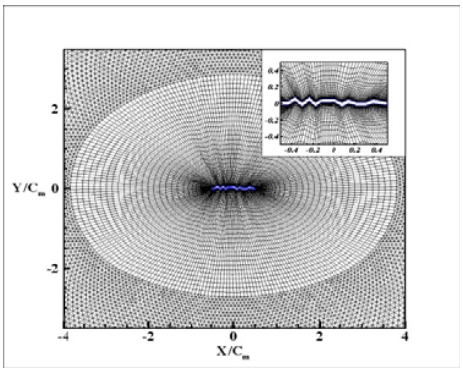

Fig. 1(a) Hybrid mesh system around the corrugated airfoil

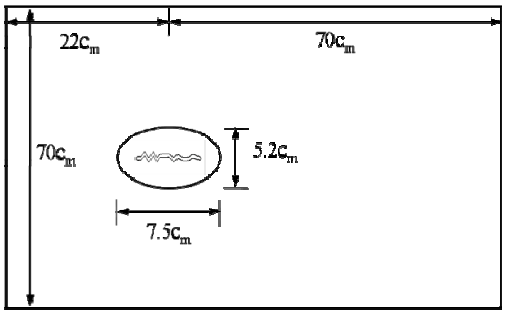

Fig. 1(b) Computational domain for the corrugated airfoil

The O-type quadrilateral cells are used to encompass the entire corrugated airfoil due to the generated aerodynamic force is dominated with the formation and separation of leading edge vortex (LEV) and trialing edge vortex (TEV) during cyclical flapping process. The dynamic motion of airfoil was dominated by external User Defined Functions (UDFs complied with C language program) during oscillated flapping motion with various inclined angle of stroke plane, stroke amplitudes and frequencies. The center of gravity is assumed at location of 0.25 times of c_m from the leading edge of airfoil. The distributions of the outer triangular cells are reconstructed according to the relative position of the flapping corrugated airfoil. The interface between the quadrilateral cells and the triangular cells is modeled by conformal type of cells to ensure the conservation of flux for all scalar variables. The outer triangular cells are smoothly re-meshed at each time interval during transient flow field simulations.

The plunge and pitch motion of the corrugated airfoil shown in Fig. 2 is respectively expressed by:

$$x(t) = \frac{A_o}{2}(1+\cos 2\pi ft)\cos\beta \qquad (3)$$

$$y(t) = \frac{A_o}{2}(1+\sin 2\pi ft)\cos\beta$$

$$\alpha(t) = \frac{\pi}{4} - \frac{\pi}{4}\sin 2\pi ft \qquad (4)$$

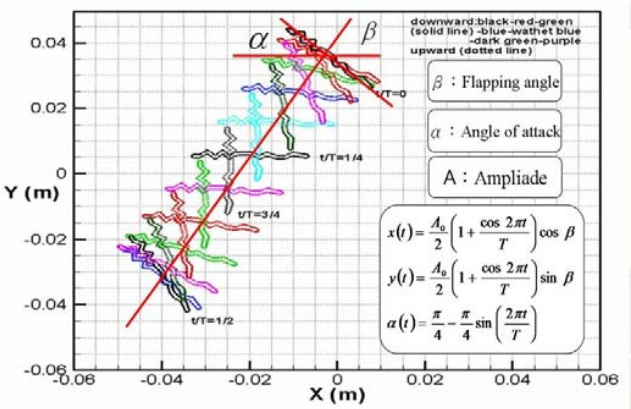

Fig. 2 Schematic view on the pre-described flapping trajectory of corrugated airfoil in up- and down-stokes.

where $x(t)$ and $y(t)$ denotes the instantaneous position of the center gravity of corrugated airfoil, A_o denotes the stroke amplitude, and f denotes the flapping frequency of corrugated airfoil. The symbol of β is the inclined angle of stroke plane. The center of pitch rotation is also located at 0.25 times of mean chord length from the leading edge of the airfoil. The initial angle of attack for corrugated airfoil is set to 45 degree for present work.

On the corrugated airfoil surface the instantaneous flow velocity is set equal to the prescribed flapping motion $[\dot{x}, \dot{y}, \dot{\alpha}]$. A no-slip boundary condition is imposed on the airfoil surface. The inflow (right side) and outflow (left side) boundary conditions are set as velocity inlet type and pressure outlet type in Fluent@ software respectively. The boundary conditions for up and down sides of grid domain are specified as symmetric planes. The initial conditions for all runs are assumed as the air flow field is rest before the corrugated airfoil starting to perform flapping motion. The ambient pressure and temperature of air is 1 atm and 25^0C respectively.

C. Design of Experiment (DOE)

Full factorial experimental design method needs a great prohibitive number of experimental calculations; however, it offers very precise results on interactions between controllable factors, with benefit of avoiding losing some information on further erroneous conclusions. The first step in the analysis of experimental design method is to identify the factors and ranges of level under investigation, which requires the theoretical understanding on unsteady flow physics of the flapping corrugated airfoil.

There are several independent operational parameters (or factors defined in DOE) influenced on the lift/thrust force generation of flapping airfoil. In order to explore the main and interaction effect of factors on obtaining the maximum lift/thrust force, the full factorial method is selected to deal with the test matrix of three factors and three levels in this work. Table I shows the design factors and level ranges considered, which are determined from open literature survey and preliminary studies. Three factors considered including of F: flapping frequency, H: stroke amplitude and S: inclined angle of stroke plane. There are 3^3=27 sets should be conducted and analysis. The main and interaction effects of three factors on the response variables (i.e. lift/thrust force) of flapping corrugated airfoil can be revealed from the runs of statistical analysis of variance (ANOVA). This is due to the F-test in ANOVA can be used to identify where the factors are significant in obtaining the maximum lift/thrust force or not. The F-value for each factor is simply a ratio of the mean of the squared deviations to the mean of the squared errors. The greater of the F-value means the significance of the factor on the maximum lift/thrust force output. In addition, the optimal combination of three tested factors and associated levels can be predicted with the larger-the-better performance characteristics and ANOVA analyses.

TABLE I
DESIGN FACTORS AND LEVELS

Factor	Symbol	Level		
		1	2	3
Flapping frequency	F	20Hz	30Hz	40Hz
Stroke amplitude	H/c_m	1.5	2.5	3
Inclined angle	S	30^o	45^o	60^o

III. RESULTS AND DISCUSSION

All the predicted results are presented and discussed with two non-dimensional aerodynamic quantities of lift force coefficient and thrust force coefficient, which are defined as:

$$C_l = \frac{F_L}{0.5\rho U_\infty^2 c_m} \quad (5)$$

$$C_t = \frac{-F_D}{0.5\rho U_\infty^2 c_m} \quad (6)$$

Since present work is interested on the aerodynamic characteristics of corrugated airfoil in forward flight, the Reynolds number is defined with forward velocity U_∞ as the reference velocity and mean chord length c_m as the reference length. The periodic solutions of C_l and C_t are obtained after at least six cycles of flapping motion when the corrugated airfoil starts from rest condition.

A. Code Validation

To validate the computer code in simulation the aerodynamic coefficients of low Reynolds number corrugated airfoil, present study performed a preliminary run on steady flow conditions of $Re = 10^4$. This is due to lack of experimental data on corrugated airfoil at $Re = 10^3$ in the open literature. Fig. 3 shows the predicted C_l/C_d curve with respect to the attack angle of airfoil. The experimental and numerical results from Kesel [20]and Vargas et al. [21]are also presented for comparison. In general, present predictions are more close to the experimental data of Kesel in comparison with those of Vargas et al. The discrepancy in lift force coefficient and drag force coefficient over tested ranges of attack angle is due to the two-dimensional model is employed in numerical run while a three-dimensional finite aspect ratio airfoil model used by Kesel in wind tunnel test. However, the predicted trend of C_l/C_d curve with increasing of attack angle of airfoil is reasonable.

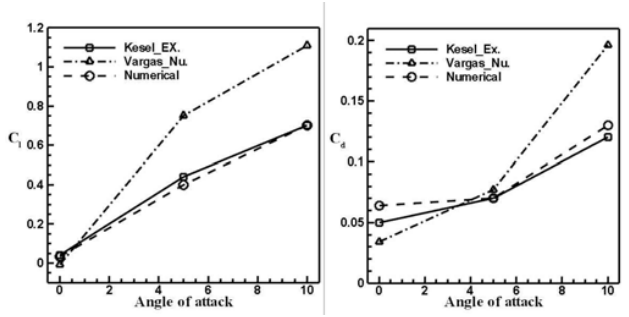

Fig. 3 The predicted C_l/C_d curve with respect to the attack

B. Unsteady Flow Mechanisms

The instant vorticity contours for corrugated airfoil over a complete cycle under $Re=10^3$, F=40Hz, $H=3.0c_m$ and $S=45^o$ are plotted in Fig. 4 for the discussion of the unsteady flow mechanism. When the airfoil started to travel into specified down-stroke positions, i.e. t=0/10T shown in Fig. 4(a), the acceleration of airfoil results in the leading edge portion of lower surface is covered by a clock-wise circulation vortex which forces the aft counter-clock-wise circulation vortex gradually moves toward the trailing edge of airfoil to produce thrust force. In the same moment, minor lift force can be observed even when the effective attack angle of airfoil is as large as 45^o. This is due to the occurrence of dynamic stall and wake capture. When the effective attack angle of airfoil decreases to zero degree, the formation of leading edge vortex (LEV) on upper surface results in visible increasing of the lift force, shown in Fig. 4(b). The net thrust force is almost zero which means that the generated thrust force from shedding TEV is balanced with the form drag and viscous drag. In period of t=0/10T to 5/10T, i.e. the down-stroke stage, the rotational circulation effect causes a local peak in the lift force curve. Fig. 4(c) shows that a large vortex pairs exists in the forward portion of upper surface of airfoil. The rotational direction of vortex in the inner part is clockwise while that in the outer part is counter-clockwise.

When the corrugated airfoil undergoes the up-stroke stage, inspections on the aerodynamic force curves reveals that there is almost no positive lift force being generated with present specified flapping motion. However, there are twin peaks in the thrust force curve. The first peak is due to the LEV on upper surface is shedding from the trailing edge of airfoil to from a reverse von Karman vortex, shown in Fig. 4(d). At instant time of t=8/10T, the corrugated airfoil is vertical from the approaching airstream, Fig. 4(e) displays that a large clockwise circulation vortex exist on the aft portion of leeward surface while a counter-clockwise vortex on the front portion of windward surface. The largest and second peak of thrust force is attributed to the appearance of these vortex pairs around the corrugated airfoil. Similar observations can be referred to other combinations of operational parameters.

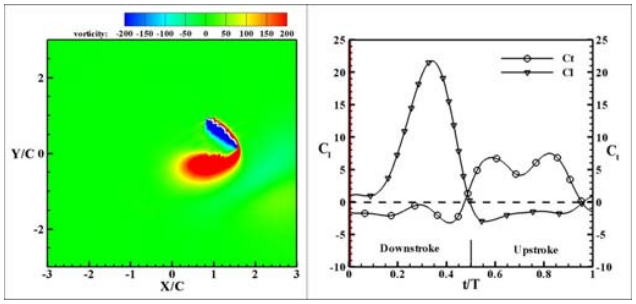

(a)t=0/10T

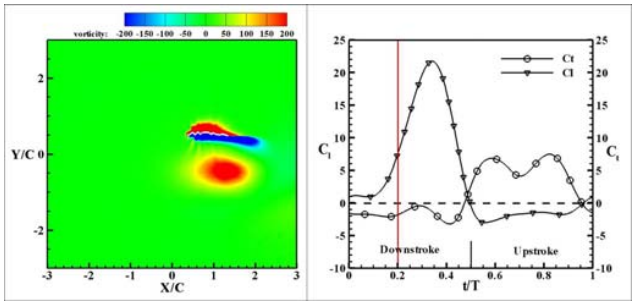

(b)t=2/10T

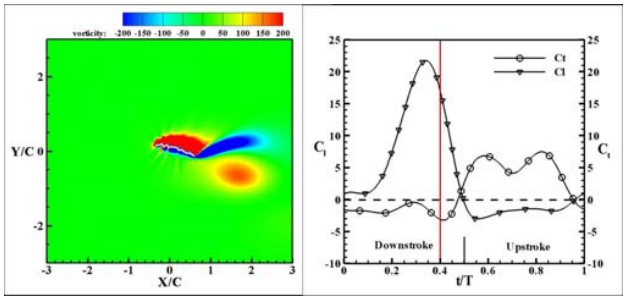

(c) t=4/10T

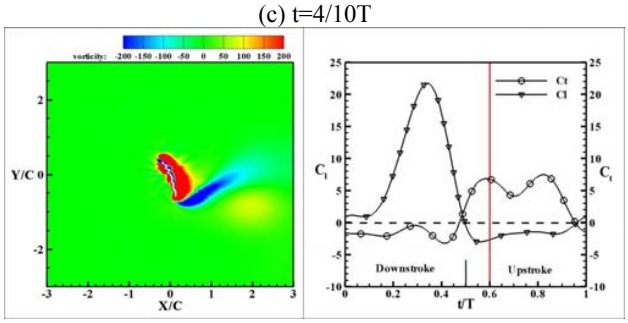

(d)t=6/10T

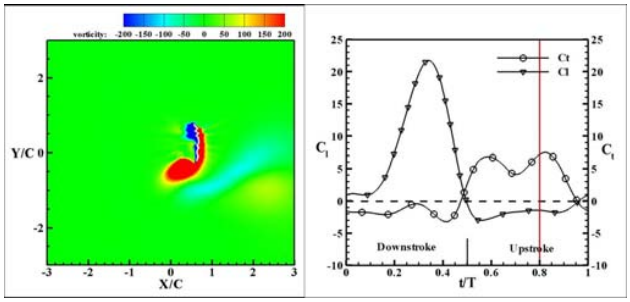

(e)t=8/10T

Fig. 4 The instant vorticity contours around a corrugated airfoil (left) and predicted C_l/C_t curve (right) over a complete flapping cycle for condition of Re=10^3, F=20Hz, H=1.5c_m and S=30^o.

C. Main Effect and Interaction between Factors

Table II lists the predicted periodic-average C_t and C_l values for all runs. The second column represents the combination of the selected operational factors and levels for evaluated the corresponding unsteady aerodynamic performance. For example, $F_1H_1S_1$ means the test case of flapping frequency, stroke amplitude, and inclined angle of stroke plane is 20 Hz, 1.5c_m (i.e. 1.5 times of mean chord length) and 30^o, respectively. The periodic-averaged data were obtained from integration of instant C_t or C_l values with flow time over at least five complete oscillation cycles then divided with the total time period. There data can be used to conduct the ANOVA analysis to find out the parameter combination of maximum C_t value and maximum C_l value, listed in Table III and Table IV respectively.

TABLE II
PREDICT PERIODIC-AVERAGED C_T AND C_L VALUES

Case Num.	Combination	C_t	C_l
1	$F_1H_1S_1$	1.376	3.141
2	$F_1H_1S_2$	0.281	2.160
3	$F_1H_1S_3$	-0.150	1.841
4	$F_1H_2S_1$	1.757	2.348
5	$F_1H_2S_2$	0.526	1.637
6	$F_1H_2S_3$	0.048	1.354
7	$F_1H_3S_1$	1.889	2.182
8	$F_1H_3S_2$	0.657	1.592
9	$F_1H_3S_3$	0.103	1.244
10	$F_2H_1S_1$	1.692	2.577
11	$F_2H_1S_2$	0.420	1.814
12	$F_2H_1S_3$	0.036	1.528
13	$F_2H_2S_1$	1.899	2.037
14	$F_2H_2S_2$	0.587	1.449
15	$F_2H_2S_3$	0.184	1.200
16	$F_2H_3S_1$	1.985	1.933
17	$F_2H_3S_2$	0.679	1.377
18	$F_2H_3S_3$	0.224	1.124
19	$F_3H_1S_1$	1.840	2.283
20	$F_3H_1S_2$	0.520	1.621
21	$F_3H_1S_3$	0.085	1.399
22	$F_3H_2S_1$	1.936	1.845
23	$F_3H_2S_2$	0.647	1.324
24	$F_3H_2S_3$	0.211	1.135
25	$F_3H_3S_1$	2.150	1.921
26	$F_3H_3S_2$	0.768	1.378
27	$F_3H_3S_3$	0.239	1.071

TABLE III
ANALYSIS OF VARIANCE FOR C_L

Source	DF	Seq SS	Adj SS	Adj MS	F	P
F	2	0.725	0.725	0.363	165.20	0.0
H	2	1.377	1.377	0.688	313.54	0.0
S	2	4.115	4.115	2.057	937.14	0.0
F*H	4	0.126	0.126	0.032	14.4	0.001
F*S	4	0.057	0.057	0.014	6.49	0.012
H*S	4	0.067	0.067	0.017	7.65	0.008
Error	8	0.018	0.018	0.002		
Total	26	6.485				

TABLE IV
ANALYSIS OF VARIANCE FOR C_T

Source	DF	Seq SS	Adj SS	Adj MS	F	P
F	2	0.208	0.208	0.103	99.28	0.0
H	2	0.386	0.386	0.193	184.35	0.0
S	2	14.42	14.42	7.21	6894.5	0.0
F*H	4	0.027	0.027	0.007	6.44	0.013
F*S	4	0.022	0.022	0.006	5.33	0.022
H*S	4	0.023	0.023	0.006	5.59	0.019
Error	8	0.008	0.008	0.001		
Total	26	15.09				

Fig. 5 and 6 respectively show the main effects of design factors on the corresponding C_t value and C_l value for $Re=10^3$. Increasing the flapping frequency from 20 Hz to 30Hz enhances the C_t value by 22.5%. Further increasing it to 40Hz enhances the C_t value by 33.3%, shown in Fig. 5. The main effect of flapping frequency on the C_l value is revered from that on the C_t value, shown in Fig. 5. Increasing the stroke amplitude has positive effect on the C_t value. This means that the thrust-indicative wake shedding from the trailing edge of airfoil has more strength with longer stroke amplitude, shown in Fig. 7(a). In the other side, increasing of stroke amplitude from $1.5c_m$ to $2.5c_m$ suppress the C_l value about 19.8%, while further increasing it to $3.0c_m$ does not obviously reduce the C_l value. This observation can be exposed from the predicted results about the effect of stroke amplitude on distribution of mean velocity in y-component, shown in Fig. 7(b). The main effect of the inclined angle of stroke plane shows that a maximum C_t and C_l value are reached for condition of flapping frequency of 20Hz. As compared with the other two factors, the flapping frequency seems to be the most significant effect on obtaining of maximum C_t and C_l value.

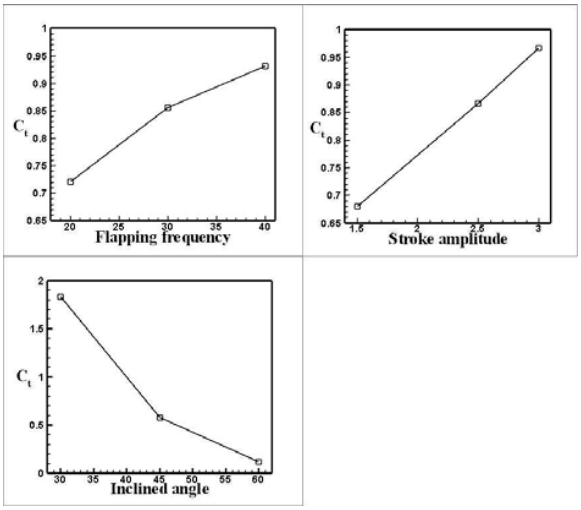

Fig. 5 Main effects plot for C_t

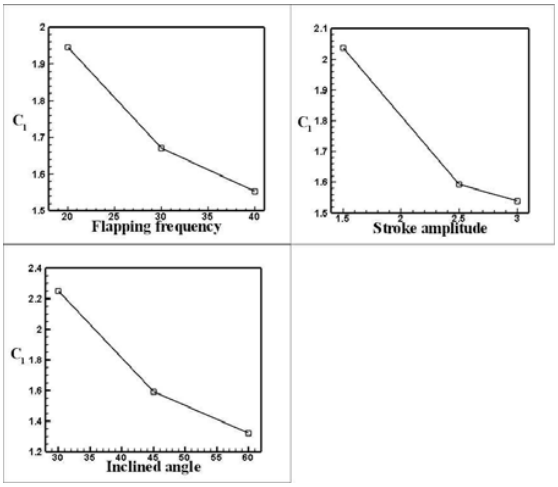

Fig. 6 Main effects plot for C_l

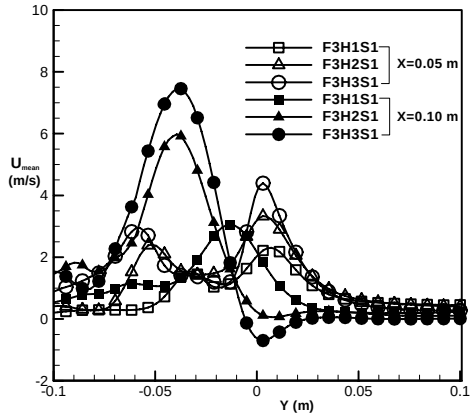

(a)

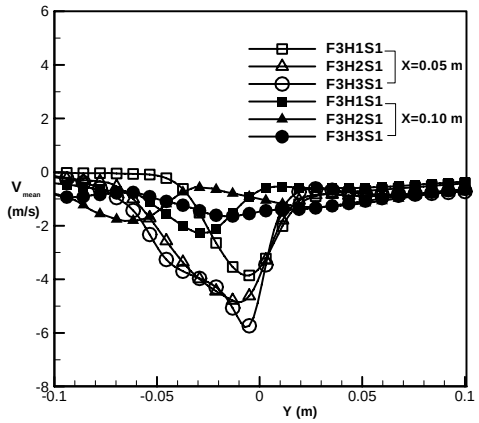

(b)

Fig. 7 The average velocity of X and Y component in Y-dir with different amplitude when the distance in 0.05m and 0.1m at the wing trailing edge section.

Among all tested runs, the combination of factors and levels

for generating of maximum thrust force coefficient and lift force coefficient is $F_3H_3S_1$ and $F_1H_1S_1$, respectively. Inspection on Fig.s 5~6, some interested observations can be discovered. For example, if the dragonfly wants to flight faster and higher above the ground, it needs not only to flap the wings with faster frequency but also with smaller stroke amplitude and inclined angle of stroke plane.

To explore the possible interaction between the factors, Fig. 8 and 9 show the interaction plots of three design factors on C_t and C_l value, respectively. Significant interaction is represented by non-parallel lines in each plot. When Fig. 8 and 9 are analyzed, it is clear that the strong interactions between the tested three factors are existing due to all lines are visible lack of parallelism. For design the flapping MAVs with corrugated wings, the optimization approach to the combination of operational parameters to obtain maximum C_t or C_l should be conducted in further.

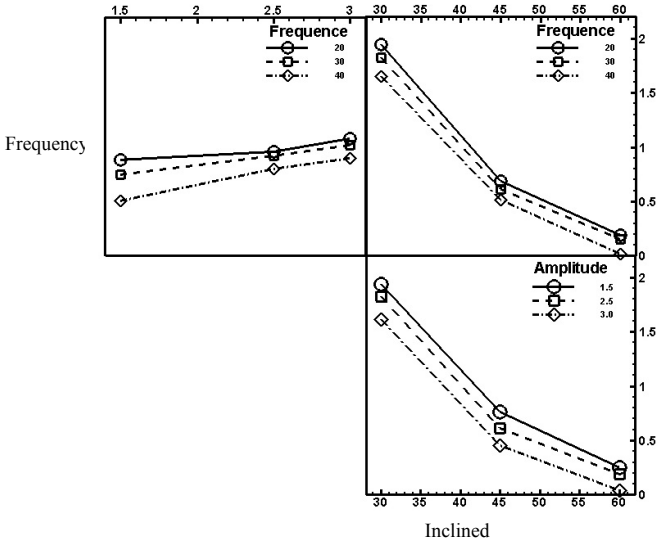

Fig. 8 Interaction plot for C_t

The flapping MAV with capacity of self-adjustable maneuver to create it flights like birds or insects is the final stage for on-field applications. Therefore, the regression models used to predict the periodic-averaged lift force and thrust force coefficient with related to the control factors such as flapping frequency, stroke amplitude, and inclined angle are also important in the building of embedded auto-pilot control unit. With the ANOVA analysis on the data from conducting of full-factorial design method, the second-order regression models for present tested corrugated airfoil to generate periodic-averaged C_t and C_l values are expressed as:

$$C_t=4.82085+0.04968\times F+0.47860\times H-0.20588\times S-0.00029\times F^2+0.00763\times H^2+0.00181\times S^2-0.00523\times F\times H-0.00021\times F\times S-0.00364\times H\times S \quad (7)$$

$$C_l=9.84122-0.1168\times F-1.9723\times H-0.13299\times S+0.00078\times F^2+0.22378\times H^2+0.00085\times S^2+0.01326\times F\times H+0.00044\times F\times S+0.00514\times H\times S \quad (8)$$

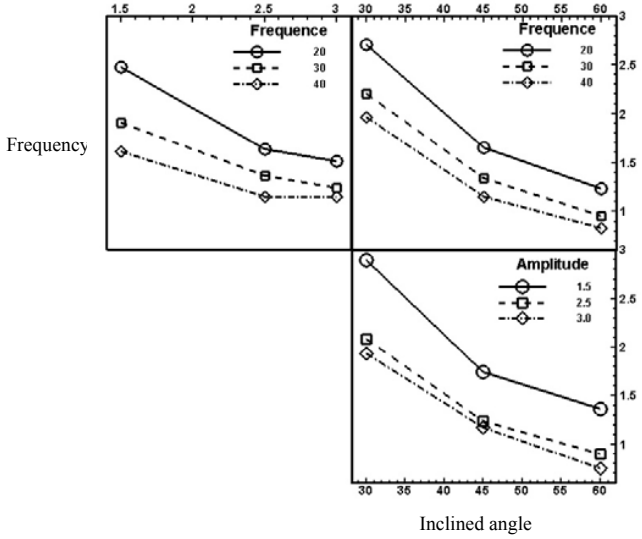

Fig. 9 Interaction plot for C_l

IV. Conclusion

Design of flapping MAVs is a complex problem because of a wide range of factors influenced on the unsteady aerodynamic performance of wings. A 3^3 full factorial design of experiments coupled with the ANOVA analysis was successfully used in this work to explore the main and interaction effect between factors on the generated lift force and thrust force as the corrugated wing undergoing the specified flapping trajectory. A two-dimensional CFD model is employed to evaluate the unsteady vortex flow mechanisms on generation of lift force and thrust force in such low Reynolds number flow field. The conformal hybrid mesh system and the dynamic mesh technique are used to model the flapping motion of a corrugated wing under various combinations of flapping frequency, stroke amplitude, and inclined angle of stroke plane. Results indicated that the inclined angle is the most significant factor on both the lift force and thrust force. There are strong interactions between tested factors. Among all tested runs, the combination of factors for maximum thrust force coefficient and lift force coefficient is $F_3H_3S_1$ and $F_1H_1S_1$, respectively.

Appendix

NOMENCLATURE

A_o = amplitude of flapping stroke

c_m = mean chord-wise length of corrugated airfoil

C_d = drag force coefficient

C_l = lift force coefficient

C_t = thrust force coefficient

f = flapping frequency

P = static pressure of flow (Pa)

Re = Reynolds number, $\rho U_\infty c_m / \mu$

t = dimensional time

T = flapping period, $2\pi/\omega$

U_∞ = free-stream velocity

x,y = Cartesian coordinate axis

β = inclined angle of stroke

ρ = density of fluid

μ = Viscosity of fluid

ω = circular frequency of flapping oscillations, $2\pi f$

ACKNOWLEDGMENT

The finical support from National Science Council of Taiwan under contract number of NSC97-2212-E-606-019 is deeply appreciated.

REFERENCES

[1] Mueller T. J. (ed.), "Fixed and Flapping Wing Aerodynamics for Micro Air Vehicle Applications". *Progress in Aeronautics and Astronautics,* 195, AIAA, Reston, VA, 2001, pp. 453-471.

[2] Triantafyllou G. S., Triantafyllou M. S. and Grosenbaugh M. A., "Optimal Thrust Development in Oscillating Foils with Application to Fish Propulsion". *Journal of Fluids and Structures,* Vol. 7, 1993, pp. 205-224.

[3] Lai, J.C.S., Platzer, M.F., "The Characteristics of a Plunging Airfoil at Zero Free-stream Velocity". *AIAA Journal,* Vol. 39, 2001, pp. 531-534.

[4] Jones, K. D., Dohring, C. M., and Platzer, M. F., "Experimental and Computational Investigation of the Knoller-Betz Effect". *AIAA Journal,* Vol. 36, No. 7, 1998, pp. 1240-1246.

[5] Anderson, J.M., Streitlien, K., Barrett, D.S., Triantafyllou, M.S., "Oscillating Foils of High Propulsive Efficiency". *Journal of Fluid Mechanics,* Vol. 360, 1998, pp. 41-72.

[6] Ellington, C. P., "The Novel Aerodynamics of Insect Flight: Applications to Micro-Air-Vehicles". *Journal of Experimental Biology,* Vol. 202, No.23, 1999, pp. 3439-3448.

[7] Dickinson, M. H., Lehmann, F. O., and Sane, S. P., "Wing Rotation and the Aerodynamic Basis of Insect Flight". *Science,* Vol. 284, 1999, pp. 1954-1960.

[8] Kawamura, Y., Soudal, S., Nishimoto, S., Ellington, C.P., Clapping-Wing Micro Air Vehicle of Insect Size. In: N. Kato, S. Kamimura (eds.) Bio-Mechanisms of Swimming and Flying, Springer Verlag, 2008.

[9] Ansari, A.A., Phillips, N., Stabler, G., Wilkins, P.C., Żbikowski, R., and Knowles, K. "Experimental Investigation of Some aspects of Insect-Like Flapping Flight Aerodynamics for Application to Micro Air Vehicles". *Exp. Fluids*, Vol. 46, 2009, pp. 777-798.

[10] Jones, K. D. and Platzer, M. F., "Design and Development Considerations for Biologically Inspired Flapping-Wing Micro Air Vehicles". *Exp. Fluids,* Vol. 46, 2009, pp. 799-810.

[11] Tuncer,I. H., Platzer, M. F., "Thrust Generation due to Airfoil Flapping". *AIAA Journal,* Vol. 34, 1996, pp. 509-515.

[12] Isogai, K., Shinmoto, Y., Watanabe, Y., "Effect of Dynamic Stall on Propulsive Efficiency and Thrust of a Flapping Airfoil". *AIAA Journal,* Vol. 37, 1999, pp. 1145-1151.

[13] Isaac, K. M., Rolwes, J., and Colozza, A., " Aerodynamics of a Flapping and Pitching Wing Using Simulations and Experiments". *AIAA Journal,* Vol. 46, 2008, pp. 1505-1515.

[14] Chandar, D., and Damodaran, M., "Computational Study of Unsteady Low Reynolds Number Airfoil Aerodynamics on Moving Overlapping Meshes," *AIAA Journal,* Vol. 46, 2008, pp. 429-438.

[15] Miao, J. M. and Ho, M. H., " Effect of Flexure on Aerodynamic Propulsive Efficiency of Flapping Flexible Airfoil". *Journal of Fluids and Structures,* Vol. 22, 2006, pp. 401-419.

[16] Miao, J. M., Sun, W. S., and Tai, C. H., "Numerical Analysis on Aerodynamic Force Generation of Biplane Counter-Flapping Flexible Airfoils". *Journal of Aircraft*, Vol. 46, No. 5, 2009, pp. 1785-1794.

[17] Wang, Z. J. " Two Dimensional Mechanism of Hovering". *Phys. Rev. Lett.,* Vol. 85, 2000, pp. 2216–2219.

[18] Wang Z. J. " The Role of Drag in Insect Hovering". *J. Exp. Biol,.*Vol. 207. 2004, pp. 4147–4155.

[19] Tamai, M., Wang, Z., Rajagopalan, G., Hu, H., and He, G., "Aerodynamic Performance of a Corrugated Dragonfly Airfoil Compared with Smooth Airfoils at Low Reynolds Number". *45th AIAA Aerospace Science Meeting and Exhibit,* Reno, Nevada, Jan 8-11, 2007.

[20] Kesel , A. B. "Aerodynamic Characteristics of Dragonfly Wing Sections Compared with Technical Aerofoils". *J. Exp. Biol*. Vol. 203, 2000, pp. 3125-3135.

[21] Vargas, A., Mittal, R., and Dong, H., "A Computational Study of the Aerodynamic Performance of a Dragonfly Wing Section in Gliding Flight". *Bioinspiration & Biomimeti*cs, Vol. 3, 2008, pp. 1-13

Jr-Ming Miao received his bachelor degree from Chung Cheng Institute of Technology in 1989 and Ph. D. degree from National Taiwan University in 1997. Afterwards, he joined the Dept. of Mechanical Engineering of Chung Cheng Institute of Technology as an associate professor. He was promoted to full professor in 2005. In August 2009, He transferred to National Pingtung University of Science and Technology to be a full professor and chairman of department of materials engineering. His research areas include CFD application on industry, micro-fluidics, PEMFC, MAV, low Reynolds number aerodynamics of flapping wing, and fluid-thermal process in cooling devices for electronic equipments, IPMC actuators. E-mail: jmmiao@mail.npust.edu.tw